Frontiers in Plant Science

TYPE Original Research
PUBLISHED 02 December 2024
DOI 10.3389/fpls.2024.1500624

OPEN ACCESS

EDITED BY
Zi-Shan Zhang,
Shandong Agricultural University, China

REVIEWED BY
Charilaos Yiotis,
University of Ioannina, Greece
Xiaolin Wang,
Chinese Academy of Agricultural Sciences,
China

*CORRESPONDENCE
Quentin Beauclaire
q.beauclaire@uliege.be

RECEIVED 23 September 2024
ACCEPTED 11 November 2024
PUBLISHED 02 December 2024

CITATION
Beauclaire Q, Vanden Brande F and Longdoz B (2024) Key role played by mesophyll conductance in limiting carbon assimilation and transpiration of potato under soil water stress.
Front. Plant Sci. 15:1500624.
doi: 10.3389/fpls.2024.1500624

Key role played by mesophyll conductance in limiting carbon assimilation and transpiration of potato under soil water stress

Quentin Beauclaire*, Florian Vanden Brande and Bernard Longdoz

BIODYNE Biosystems Dynamics and Exchanges, TERRA Teaching and Research Center, Gembloux Agro-Bio Tech, University of Liege, Gembloux, Belgium

Introduction: The identification of the physiological processes limiting carbon assimilation under water stress is crucial for improving model predictions and selecting drought-tolerant varieties. However, the influence of soil water availability on photosynthesis-limiting processes is still not fully understood. This study aimed to investigate the origins of photosynthesis limitations on potato (*Solanum tuberosum*) during a field drought experiment.

Methods: Gas exchange and chlorophyll fluorescence measurements were performed at the leaf level to determine the response of photosynthesis-limiting factors to the decrease in the relative extractable water (REW) in the soil.

Results: Drought induced a two-stage response with first a restriction of CO_2 diffusion to chloroplasts induced by stomatal closure and a decrease in mesophyll conductance, followed by a decrease in photosynthetic capacities under severe soil water restrictions. Limitation analysis equations were revisited and showed that mesophyll conductance was the most important constraint on carbon and water exchanges regardless of soil water conditions.

Discussion: We provide a calibration of the response of stomatal and non-stomatal factors to REW to improve the representation of drought effects in models. These results emphasize the need to revisit the partitioning methods to unravel the physiological controls on photosynthesis and stomatal conductance under water stress.

KEYWORDS

modeling, photosynthesis, stomata, drought, partitioning, potato, mesophyll

1 Introduction

European ecosystems are facing more intense and frequent water stress events due to altered rainfall patterns and rising temperatures induced by anthropogenic climate change (Samaniego et al., 2018). Precipitation shortage episodes perturbate plant water status and induce disruptions of the water and carbon cycles through the inhibition of carbon assimilation and transpiration (Bertolino et al., 2019; Fahad et al., 2017; Trenberth et al., 2014). As a result, ecosystem services such as food production and carbon storage are strongly impacted by the lack of soil water (Chang and Bonnette, 2016; Hendrawan et al., 2022; Kang et al., 2021). Land–atmosphere feedbacks originating from the perturbation of such processes may exacerbate climate change through water stress intensification (Anderegg et al., 2019; Hartick et al., 2022). An in-depth understanding of the effects of drought on plant physiology is required to predict future ecosystem service capacities and to improve climate model predictions (Ryu et al., 2019).

Photosynthesis is the process by which plants convert CO_2 into carbohydrates. Carbon assimilation is mediated by the physiological barriers on the CO_2 diffusion pathway (i.e., stomatal opening and diffusion within the mesophyll; Gago et al., 2020; Nadal and Flexas, 2018) and by the Rubisco efficiency for fixing CO_2 in the Calvin cycle (Farquhar et al., 1980). Uncertainties remain on the importance of each limiting factor under soil water-limiting conditions (Rogers et al., 2017).

Quantifying the importance of photosynthesis-limiting factors under drought is also pivotal for assessing phenotype plasticity and selecting drought-tolerant plant species (Lupo and Moshelion, 2024; Nguyen et al., 2023). To that end, mechanistic modeling can be used to disentangle the complexity of the mechanisms regulating plant response to water stress (Stirbet et al., 2020). In the Farquhar–von Caemmerer–Berry (FvCB) model (Farquhar et al., 1980), carbon assimilation under high irradiance (A_{sat}) is constrained by stomatal conductance (g_s), mesophyll conductance (g_m), and the maximum carboxylation rate of Rubisco (V_{cmax}). The quantitative contribution of each of these factors in limiting photosynthesis under water stress can be estimated by, first, writing the total derivative of A_{sat} as a sum of the total derivative of these factors and, second, by estimating the response of these factors to soil water availability. This method, also known as limitation analysis (Grassi and Magnani, 2005; Jones, 1985), can be used to partition photosynthesis limitations between stomatal (i.e., a decrease in A_{sat} originating from g_s) and non-stomatal factors (i.e., a decrease in A_{sat} originating from g_m and/or V_{cmax}).

Stomata are the gates of CO_2 diffusion and water transpiration at the leaf surface. Stomatal opening is regulated by a complex interplay of abiotic and biotic factors. For instance, it is well known that an increase in vapor pressure deficit (VPD) drives the closure of stomata through the evaporation of water in the guard cells (McAdam and Brodribb, 2016). In addition, carbon assimilation regulates stomatal opening to balance the CO_2 diffusion with the efficiency of the Calvin cycle (Wong et al., 1979). A mechanistic formulation of these relationships was proposed by Cowan and Farquhar (1977), who hypothesized that stomatal opening is regulated to maximize carbon gains and minimize water losses over a constant time interval. This optimization theory is at the basis of the unified stomatal optimality (USO) model where g_s is expressed as a function of VPD, CO_2 concentration at the leaf surface, carbon assimilation, and the stomatal sensitivity to photosynthesis (g_1) (Medlyn et al., 2011). This last, which is the slope of the USO model (g_1), is linked to the water use strategy of the plant by being inversely proportional to the marginal carbon cost of water (Medlyn et al., 2011). During drying-up episodes, short timescale variations of g_1 can be used as an indicator of plants' adaptation strategy. In the framework of the optimality theory, plants can maximize carbon gains (increase in g_1), minimize water losses (decrease in g_1), or keep the same balance between carbon gains and water losses (constant g_1). The response of g_1 to soil water availability is likely species or plant functional type (PFT)-specific (Beauclaire et al., 2023; Gourlez de la Motte et al., 2020; Héroult et al., 2013; Zhou et al., 2013). Although the formulation of the relationship between g_s and A_{sat}, and the water cost associated with the opening of stomata are still active research topics in the scientific community (Lamour et al., 2022; Mrad et al., 2019), the USO model has become a reference for representing stomatal behavior in land surface models (LSMs) (Kala et al., 2015; Lawrence et al., 2019; Sabot et al., 2022).

As g_s is mediated by carbon assimilation, a decrease in g_s can also be induced by biochemical or mesophyll limitations, which regulate stomatal opening with the mesophyll demand for CO_2 (Lemonnier and Lawson, 2023; Medlyn et al., 2011; Zhou et al., 2013). As a result, g_s and A_{sat} are strongly coupled, and stomatal closure can originate either from an optimal stomatal adaptation or from a disguised effect of mesophyll conductance and/or carboxylation rate of Rubisco (Medlyn et al., 2011; Zhou et al., 2013). This feedback effect complicates the identification of the origins of stomatal closure and photosynthesis limitations under water stress. Using g_1 as evidence of optimal stomatal control on photosynthesis theoretically allows to identify the feedback effect of non-stomatal factors on stomatal closure by linking photosynthesis limitations to the stomatal optimality theory (Zhou et al., 2013). As a result, coupling the USO and FvCB models in the limitation analysis would enable a quantitative assessment of the effects of g_1, VPD, g_m, and V_{cmax} on g_s and A_{sat}. To our knowledge, this study is the first to develop this approach. The limitations of photosynthesis originating from stomatal closure induced by a decrease in g_1 or g_s are further referred to as a stomatal origin limitation (SOL), while an effect of g_m and/or V_{cmax} is referred to as a non-stomatal origin limitation (NSOL) (Beauclaire et al., 2023; Gourlez de la Motte et al., 2020).

Soil water content (SWC) is a key eco-hydrological variable impacting plant metabolism and more globally carbon and water fluxes (Zhou et al., 2021). In particular, lack of soil water triggers complex mechanisms which regulate the water flow in the plant to avoid hydraulic failure (Martínez-Vilalta et al., 2014). When soil edaphic proprieties are known, SWC can be used to determine the relative extractable water (REW) for plant uptake (Granier et al., 2007), which is often used in LSMs as a drought index to implement water stress effects on photosynthesis originating from either SOL or NSOL (Vidale et al., 2021). The response of FvCB and USO model parameters to decreasing soil water availability strongly differs across PFTs, which makes REW a critical variable for modeling the response of terrestrial ecosystems to drought (Peters et al., 2018; Rogers et al., 2017; Vidale et al., 2021; Zhou et al., 2013).

Potato is one of the most important crops, providing food for more than one billion people around the world (Lutaladio and Castaldi, 2009). In Europe, more than 400,000 hectares of arable land are used for potato cultivation (Goffart et al., 2022). This crop are highly sensitive to water stress because of its shallow root system and its inability to extract water from deeper soil layers (Obidiegwu, 2015). In particular, tuber bulking is a critical stage of potato growth, as it determines the yield and quality of the harvest (Gervais et al., 2021). Partitioning photosynthesis limitations is crucial for selecting drought-tolerant varieties and ensuring food security. We have implemented this approach during a drought experiment on field-grown potatoes. The goals of this study were i) to describe the response of A_{sat}, g_s, g_m, g_1, and V_{cmax} to the decrease in REW; ii) to perform a limitation analysis on A_{sat} using g_s or g_1, g_m, V_{cmax}, and VPD as explanatory variables; and finally iii) to define REW thresholds from which each of these limitations occurred.

2 Material and methods

2.1 Plant materials and experimental setup

Potato plants were grown on a 4-ha experimental land located in Belgium, approximately 50 km southeast of Brussels (50°33′47.772″ N, 4°42′46.403″E). This cropland is usually used for cultivating chicory, sugar beet, and winter wheat. In total, 88 tubers of potato (*Solanum tuberosum*, cv Agria) were planted under a plastic polytunnel greenhouse 12m long and 5m wide.

SWC and soil temperature were measured using time domain reflectometers (ML3 ThetaProbe, Delta-T Devices Ltd., Cambridge, UK) placed at depths of 10 cm and 30 cm. Air humidity and air temperature were measured using a resistive platinum thermometer and electrical capacitive hygrometer (HMP155, Vaisala Oyj, Helsinki, Finland) placed under the plastic tunnel at 1.5-m height. The tubers were planted on May 15, 2020, and the first leaves appeared on June 4, 2020, which were considered the emergence [i.e., day after emergence (DAE) of 0].

Soil water availability was quantified by calculating the REW of the first soil horizon, where most of the root water uptake of potato is expected to occur (Beauclaire et al., 2023):

$$REW = \left\{ \frac{\theta_{H1} - \theta_{wp,H1}}{\theta_{fc,H1} - \theta_{wp,H1}} \right. \tag{1}$$

where $\theta_{wp,H1}$ = 15.6 and $\theta_{fc,H1}$ = 35.01 (cm^3 cm^{-3}) are respectively the wilting point and the field capacity of the first horizon (H_1: 0–30 cm) and θ_{H1} is the SWC measured in H_1, which was calculated as the weighted mean of SWC measurements at depths of 10 cm and 30 cm (with a weight of 2/3 and 1/3, respectively). $\theta_{wp,H1}$ and $\theta_{fc,H1}$ were estimated from soil water retention curves using the van Genuchten (VG) model (van Genuchten, 1980). Soil samples were collected before the experiment at a 15cm depth (three replicates) and were saturated for at least 24 h in distilled water. The pressure plate method (Richards, 1948—following the ISO 11274 standard) was applied, and the measurements of the suction head and SWC were recorded. $\theta_{wp,H1}$ and $\theta_{fc,H1}$ were estimated as the SWC at a pF (log of the suction head) of 4.2 and 2.0, respectively. VG model parameters and retention curves of the three soil samples are given in the Supplementary Material (Supplementary Figure S1).

Over a first period of 35 days, all the plants were hand-watered to ensure that θ_{H1} remained near field capacity. The drought treatment consisted in withholding irrigation to simulate a long-term precipitation deficit on half of the plants. The other half was hand-watered during the experiment. The drought treatment started on DAE 40 (corresponding to the beginning of the tuber bulking stage) and stopped on DAE 74 (corresponding to the appearance of the first signs of senescence on the irrigated plants). All plants experienced the same photosynthetic photon flux density (PPFD) in the photosynthetic active radiation (PAR), temperature, and VPD conditions under the plastic tunnel.

2.2 Leaf-level measurements

Gas exchange and chlorophyll fluorescence measurements were conducted during the tuber bulking stage at 14 different dates (between DAE 35 and DAE 74; Figure 1) from 10 a.m. to 4 p.m. Only the youngest leaves in the upper part of the plant were selected by randomly sampling irrigated and non-irrigated plants. Measurements were performed using a LI-COR LI-6400 equipped with a LI-6400-40 fluorescence chamber (LI-COR Inc., Lincoln, NE, USA). The following procedure was applied to each leaf sample. The CO_2 concentration in the chamber (C_s) was set to 400 µmol mol^{-1}, the PPFD in the PAR was set to 1,200 µmol m^{-2} s^{-1}, and the air humidity and temperature were maintained at ambient levels. After stabilization of the steady-state fluorescence signal (F_s), a multiphase flash with a saturation light of 9,000 µmol m^{-2} s^{-1} was applied, and the maximum fluorescence intensity under the light (F_m') was measured. In addition, A_{sat}, leaf temperature, stomatal conductance to water vapor (g_{sw}), CO_2 concentration in sub-stomatal cavities (C_i), and the vapor pressure deficit at the leaf surface (VPD_{leaf}) were recorded. Stomatal conductance to CO_2 (g_s) was calculated by dividing g_{sw} by 1.6.

2.2.1 NSOL: V_{cmax} and g_m

V_{cmax} was determined using a single measurement of gas exchanges at light saturation (De Kauwe et al., 2016; Wilson et al., 2000):

$$V_{cmax} = A_{sat} \frac{C_c + K_m}{C_c - \Gamma^*} \tag{2}$$

where K_m is the Michaelis–Menten coefficient, Γ^* the CO_2 compensation point, and C_c the CO_2 concentration in the chloroplast. Equation 2 is based on a single measurement of CO_2 assimilation at light saturation instead of using CO_2-response curves, where V_{cmax} retrieval is impacted by the sensitivity of the fitting method (Miao et al., 2009). Moreover, leaf respiration (R_d) was neglected, as it is much smaller than A_{sat} (Knauer et al., 2018;

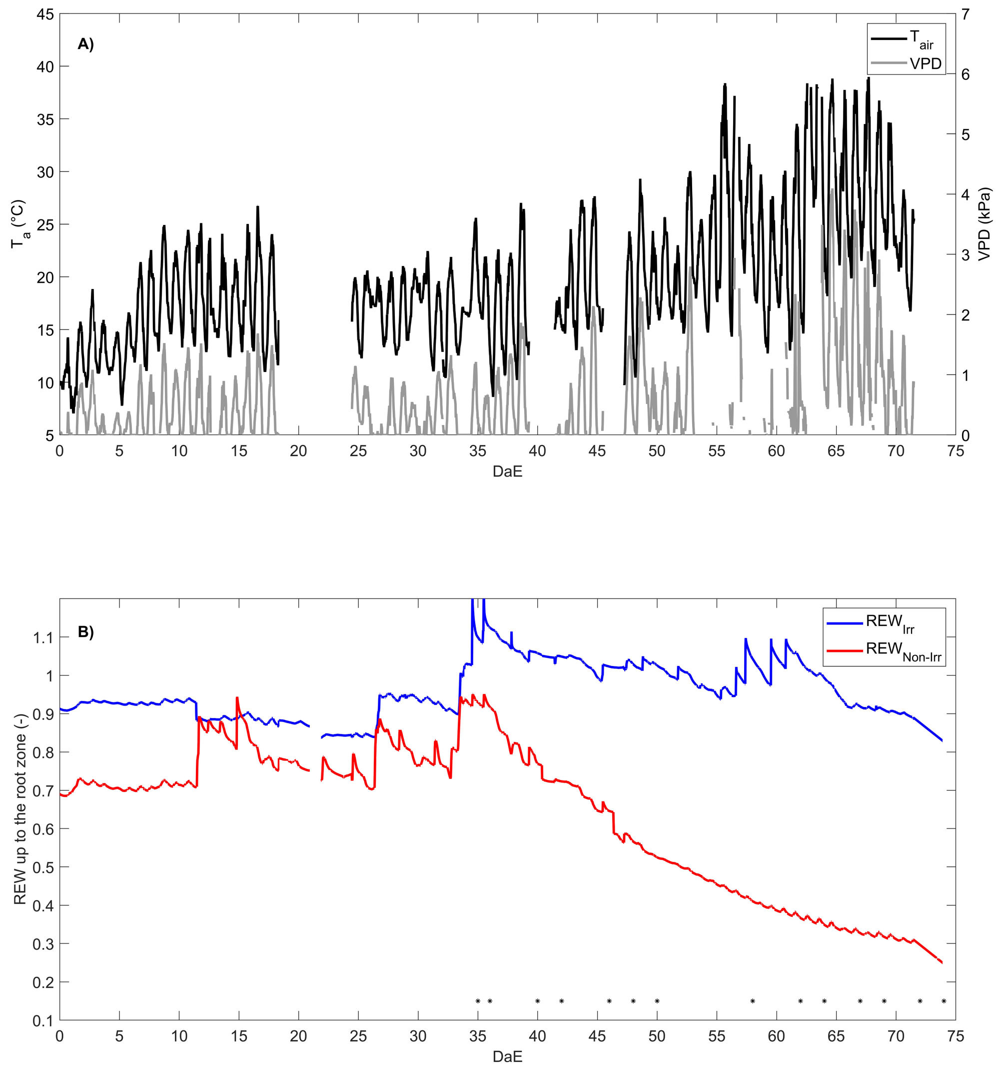

FIGURE 1
Temporal evolution of air temperature (T_{air}) and air vapor pressure deficit (VPD) under the plastic polytunnel greenhouse **(A)** and relative extractable water (REW) of the irrigated plot (REW_{irr}) and non-irrigated plot ($REW_{non-irr}$) **(B)**. The asterisk indicates the days when leaf-level measurements were conducted. DaE is day after emergence.

Von Caemmerer, 2013). K_m and Γ^* were estimated using C3 plant-based temperature response curves (Bernacchi et al., 2001). C_c was calculated using the Fick law (Farquhar and Sharkey, 1982):

$$C_c = C_i - \frac{A_{sat}}{g_m} \tag{3}$$

where g_m is determined using the "variable electron transport" method (Harley et al., 1992):

$$g_m = \frac{A_{sat}}{C_i - \frac{\Gamma^* (J_F + 8A_{sat})}{J_F - 4A_{sat}}} \tag{4}$$

where J_F is the electron transport rate estimated from PPFD, α the leaf absorptance in the PAR, φ_{PSII} the photochemical efficiency of PSII open centers, and β_{PSII} the fraction of the absorbed PAR allocated to PSII (Genty et al., 1989; Valentini et al., 1995):

$$J_F = \alpha \cdot \beta_{PSII} \cdot \varphi_{PSII} \cdot PPFD \tag{5}$$

In Equation 5, φ_{PSII} was determined from F'_m and F_s (Kramer et al., 2004):

$$\varphi_{PSII} = \frac{F'_m - F_s}{F'_m} \tag{6}$$

and $\alpha \cdot \beta_{PSII}$ was determined from the linear relationship between φ_{PSII} and the apparent quantum efficiency of the linear electron transport φ_{e-} (Valentini et al., 1995):

$$\alpha \cdot \beta_{PSII} = \frac{4}{k} \tag{7}$$

where 4 is the number of electrons needed per CO_2 molecule fixed and k the slope of the linear relationship between φ_{e-} and φ_{PSII}. Under non-photorespiratory conditions, φ_{e-} can be estimated by the apparent quantum efficiency of CO_2 uptake φ_{CO2}, which is obtained by dividing the net CO_2 assimilation by the incident PAR (Genty et al., 1989). Non-photorespiratory conditions were set by adding pure N_2 (1% O_2) into the LI-COR LI-6400 chamber. The meteorological conditions were maintained at ambient levels, and the incoming PPFD was set to the following values: 2,000, 1,500, 1,200, 1,000, 800, 600, 400, 200, 100, and 0 μmol m^{-2} s^{-1}. Gas exchanges and fluorescence intensities were measured for each PPFD value. φ_{CO2} was calculated as the ratio of net carbon assimilation to PAR. The slope of fitted linear relationship between φ_{CO2} and φ_{e-} (k) was used to determine $\alpha \cdot \beta_{PSII}$ using Equation 7. These measurements were conducted on three leaf samples for irrigated and non-irrigated plants and were repeated three times during the drought treatment (i.e., DAEs 42, 64, and 73).

2.2.2 SOL: g_s and g_1

In the USO model, g_s is a function of VPD_{leaf}, C_s, and A_{sat} (Medlyn et al., 2011):

$$g_s = \left(1 + \frac{g_1}{\sqrt{VPD_{leaf}}}\right)\frac{A_{sat}}{C_s} \tag{8}$$

where the minimum stomatal conductance is neglected under high irradiance (Medlyn et al., 2017), and g_1 is the stomatal sensitivity to photosynthesis, which is inversely related to the marginal water use efficiency (WUE) (Medlyn et al., 2011). g_1 can be determined by combining the Fick law describing the CO_2 diffusion through stomata with Equation 8, which gives (Medlyn et al., 2017)

$$g_1 = \frac{\frac{C_i}{C_s}\sqrt{VPD_{leaf}}}{1-\frac{C_i}{C_s}} \tag{9}$$

2.3 Statistical analysis

g_m values were discarded when C_i was outside of the range 150–350 μmol mol^{-1}, which minimizes errors in R_d and Γ^* and by extension in g_m (Harley et al., 1992; Niinemets et al., 2006; Veromann-Jürgenson et al., 2017). Moreover, V_{cmax} and g_m were normalized at 25°C ($V_{cmax,25}$, $g_{m,25}$) using the Arrhenius temperature response function parameterized on tobacco (Bernacchi et al., 2002, 2001). Gas exchange and chlorophyll fluorescence-related variables (i.e., A_{sat}, g_s, $g_{m,25}$, g_1, and $V_{cmax,25}$) were averaged for each day of measurement and drought treatment (irrigated and non-irrigated), thus regrouping measurements performed under similar meteorological and edaphic conditions.

The response of A_{sat}, g_s, $g_{m,25}$, g_1, and $V_{cmax,25}$ to the decrease in REW was assessed using a linear-plateau model, which consists in a constant value (y_{max}) and a linear segment (with slope a and intercept b) on either side of a threshold (REW_{th}). Such model has already been used to describe the response of SOL and NSOL to soil water availability of potato crops at the ecosystem scale (Beauclaire et al., 2023) and is used to implement the response of LSM parameters to drought (Vidale et al., 2021). The statistical significance of the linear-plateau model was assessed by comparing its Akaike information criterion corrected for low sample size (AICc; Burnham et al., 2002) to the one of a higher parsimonious model (i.e., a linear model with one slope and intercept). The model with the lowest AICc explains the greatest amount of variation while being the more parsimonious (Burnham et al., 2011; Scoffoni et al., 2012). Differences between models were considered meaningful when their AICcs differed by at least 7 (Burnham et al., 2011). If the difference was less than 7, the segmented model was selected, as such a relationship has already been observed for potato (Beauclaire et al., 2023). Model performance was assessed using the coefficient of determination (R^2) and the standard deviation (SD) of fitted parameters. The segmented regression was fitted using the "nlsm" function from the "nlraa" package in R Studio (Archontoulis and Miguez, 2015; Miguez, 2023). Statistical difference between REW_{th} parameters was tested by calculating the p-value of a t-test using the fitted values and their corresponding standard deviation (Clogg et al., 1995; Paternoster et al., 1998).

2.4 Limitation analysis

The first limitation scheme used in this study was proposed by Jones (1985), where SOL was associated to a decrease in g_s caused by a decrease in either V_{cmax} or g_m. The relative variation of A_{sat} compared to its maximum value $\frac{dA_{sat}}{A_{sat}}$ is written as the sum of the relative variations of g_s, g_m, and V_{cmax}, as follows (Grassi and Magnani, 2005; Jones, 1985):

$$\frac{dA_{sat}}{A_{sat}} = \frac{dg_s}{g_s}l_{gs} + \frac{dg_m}{g_m}l_{gm} + \frac{dV_{cmax}}{V_{cmax}}l_{Vcmax} = L_{gs} + L_{gm} + L_{Vcmax} \tag{10}$$

$$l_{gs} = \frac{\frac{g_t}{g_s}\frac{\delta A_{sat}}{\delta C_c}}{g_t + \frac{\delta A_{sat}}{\delta C_c}} \tag{11}$$

$$l_{gm} = \frac{\frac{g_t}{g_m}\frac{\delta A_{sat}}{\delta C_c}}{g_t + \frac{\delta A_{sat}}{\delta C_c}} \tag{12}$$

$$l_{Vcmax} = \frac{g_t}{g_t + \frac{\delta A_{sat}}{\delta C_c}} \tag{13}$$

where l_{gs}, l_{gm}, and l_{Vcmax} are respectively the relative stomatal, mesophyll, and biochemical limitations (corresponding to dimensionless quantity between 0 and 1 that gives the proportion of the total limitation), and L_{gs}, L_{gm} , and L_{Vcmax} are the contributions of respectively the stomatal, mesophyll, and biochemical limitations to the relative variation of A_{sat}. g_t is the total conductance to CO_2 diffusion ($g_t^{-1} = g_s^{-1} + g_m^{-1}$), and $\delta A_{sat}/\delta C_c$ is the partial derivative of A_{sat} with respect to C_c calculated using Equation 2. In this study, Equation 10 was normalized by dA_{sat}/A_{sat} to improve the interpretation of the data. The temporal dynamics of these relative variations can be explained solely by REW and VPD, as the relationship to temperature was already considered by normalizing V_{cmax} and g_m at 25°C, as well as the one to solar radiation by collecting the data at light saturation.

This approach has two drawbacks. First, the decrease in A_{sat} originating from stomatal closure through a decrease in g_s can be induced by g_m and V_{cmax}, which may result in the underestimation of the contribution of non-stomatal factors in limiting photosynthesis. Second, identifying the contribution of REW to the variation in L_{gs} is complex, as VPD has varied during the experiment. To tackle this issue, we used g_1 instead of g_s as SOL. This allows first, to separate the feedback effect of NSOL on stomatal conductance and, second, to consider the effect of VPD on stomatal closure (Zhou et al., 2013). As a result, Equation 10 was modified by calculating the total derivative of g_s using the USO model, which gives (derived in Supplementary Method S1):

$$\frac{dA_{sat}}{A_{sat}} = \frac{dg_1}{g_1}\left(\frac{l_{gs}}{1-l_{gs}}\frac{C_i}{C_s}\right) + \frac{dg_m}{g_m}\left(\frac{l_{gm}}{1-l_{gs}}\right) + \frac{dV_{cmax}}{V_{cmax}}\left(\frac{l_{Vcmax}}{1-l_{gs}}\right) - \left(\frac{1}{2}\frac{l_{gs}}{1-l_{gs}}\frac{C_i}{C_s}\right)\frac{dVPD}{VPD} \quad (14)$$

$$\frac{dA_{sat}}{A_{sat}} = \frac{dg_1}{g_1} l_{g1,USO} + \frac{dg_m}{g_m} l_{gm,USO} + \frac{dV_{cmax}}{V_{cmax}} l_{Vcmax,USO} + l_{VPD,USO}\frac{dVPD}{VPD} \quad (15)$$

$$\frac{dA_{sat}}{A_{sat}} = L_{g1,USO} + L_{gm,USO} + L_{Vcmax,USO} + L_{VPD,USO} \quad (16)$$

where $L_{g1,USO}$, $L_{gm,USO}$, $L_{Vcmax,USO}$, and $L_{VPD,USO}$ are the contributions of respectively the optimal stomatal, mesophyll, biochemical, and VPD limitations to the relative variation of A_{sat} using the USO model of stomatal conductance. Equations 15, 16 show that dA_{sat}/A_{sat} can be written as the sum of the relative variations of g_1, g_m, V_{cmax}, and VPD. Combining Equations 16, 10 allows to identify the effect of g_m, V_{cmax}, g_1, and VPD on the contribution of stomatal closure to photosynthesis, as follows:

$$L_{gs} = L_{gm,USO} - L_{gm} + L_{Vcmax,USO} - L_{Vcmax} + L_{VPD,USO} + L_{g1,USO} \quad (17)$$

$L_{gm,USO} - L_{gm} + L_{Vcmax,USO} - L_{Vcmax}$ is the effect of NSOL on stomatal closure, while $L_{VPD,USO} + L_{g1,USO}$ is the effect of VPD and g_1 on stomatal closure according to the USO model. The relative variations in Equations 10, 15 are calculated from the difference between the value of the variable at a specific REW and the asymptote of the linear-plateau using $dy/y = (y_{max} - y)/(y_{max} - min(y))$, with y being the ordinate at a specific REW value and y_{max} the plateau of the segmented regression. In a similar fashion, $dVPD/VPD$ is determined from the VPD–REW relationship. During precipitation shortage episodes, this relationship is decreasing (i.e., increase in VPD when REW decrease), which was observed during the experiment (Supplementary Figure S2). This relationship was confirmed by the data of the nearby eddy covariance station of Lonzée for similar edaphic proprieties (data not shown). Therefore, this linear relationship was used to determine $dVPD/VPD$ at each REW value.

In Equation 14, the ratio C_i/C_s also plays an important role in the limitation analysis, as it directly influences $L_{g1,USO}$ and $L_{VPD,USO}$. Using g_1 as SOL implies that any stomatal constraint on A_{sat} should be associated with an increase of the ratio A_{sat}/g_s. Indeed, following the USO model framework, this constraint corresponds to a maximization of photosynthesis while minimizing water losses. As g_s and A_{sat} both regulate CO_2 diffusion through stomatal apertures and CO_2 fixation in the chloroplasts, the increase in A_{sat}/g_s is linked to a decrease in C_i/C_s, illustrating an optimal stomatal control ($C_i/C_s \sim 1 - A_{sat}/g_s$). The relationship between C_i/C_s and REW was also evaluated by fitting a linear-plateau model as described in section 2.4. Note that $L_{VPD,\ USO}$ is per essence negative because of the partial derivative of VPD with respect to A_{sat}, as they are inversely related (i.e., VPD at the denominator in the USO model; Equation 8). As a result, any increase in VPD induces a closure of stomata and a decrease in A_{sat}. A decrease in V_{cmax}, g_m, or g_1 induces a decrease in A_{sat} for all the other terms of Equation 16.

3 Results

3.1 Meteorological and edaphic conditions

The decline in soil water availability was synchronized with a period of progressive increase in VPD and air temperature under the plastic polytunnel greenhouse (Figure 1A) up to a maximum value of 4.10 kPa and 39.02°C, respectively (Figure 1A). Both irrigated and non-irrigated plants faced an increase in atmospheric dryness and air temperature. The REW of the non-irrigated plants decreased after stopping the irrigation and reached 0.24 at the end of the experiment, while the REW of the irrigated plants remained higher than 0.83 due to continuous hand watering (Figure 1B).

3.2 Response of gas exchanges and chlorophyll fluorescence to drought

$\alpha \cdot \beta_{PSII}$ was not significantly different between irrigated and non-irrigated leaf samples at each DAE and during the experiment (Supplementary Figure S3). Therefore, the mean of all $\alpha \cdot \beta_{PSII}$ measurements was used in Equation 5 (i.e., $\alpha \cdot \beta_{PSII} = 0.73 \pm 0.08$). The linear-plateau model had the lowest AICc compared to the linear model for representing the dependence of $V_{cmax,25}$, g_1, and C_i/C_s on REW. For g_s, $g_{m,25}$, and A_{sat}, the difference between the AICc of the segmented and the linear model was less than 7 (Supplementary Table S1). Therefore, these differences were not considered significant, and the segmented model was chosen for reproducing the response of A_{sat}, C_i/C_s, g_s, $g_{m,25}$, and g_1 to REW (Figure 2, Table 1). The REW thresholds at which A_{sat}, g_s, and $g_{m,25}$ started to decrease were higher than those of $V_{cmax,25}$, g_1, and C_i/C_s (Figure 2, Table 1), which is confirmed by the p-values of the tests comparing these parameters (Table 2). Overall, CO_2 diffusion factors (i.e., $g_{m,25}$ and g_s) were the first variables to decrease with REW, while biochemical factors (i.e., $V_{cmax,25}$) were only impacted by severe REW restrictions. Because of a non-significant difference, the REW thresholds for $g_{m,25}$ and g_s were averaged, corresponding to $REW_{th,gs,gm} = 0.72 \pm 0.12$. Biochemical limitation ($V_{cmax,25}$) was only negatively impacted by severe soil water restrictions ($REW_{th,Vcmax} = 0.43 \pm 0.04$). g_1 and C_i/C_s increased from a smaller REW threshold compared to $V_{cmax,25}$ ($REW_{th,\ g1,CiCs} = 0.37 \pm 0.02$; Figure 2, Tables 1, 2).

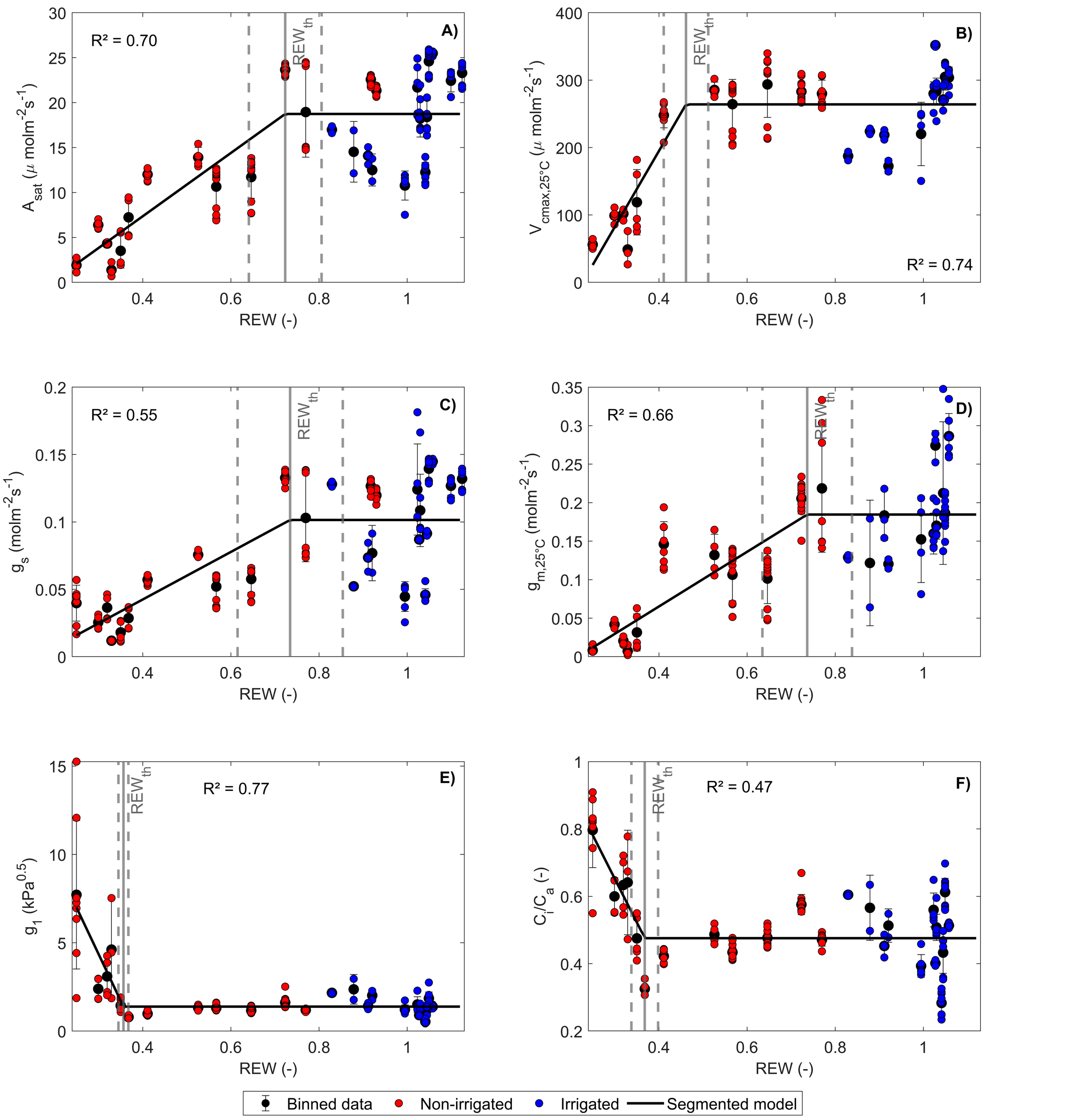

FIGURE 2
Response of A_{sat} **(A)**, $V_{cmax,25}$ **(B)**, g_s **(C)**, $g_{m,25}$ **(D)**, g_1 **(E)**, and C_i/C_s **(F)** to relative extractable water (REW). Red and blue dots indicate respectively non-irrigated and irrigated potato plants. The fitted curve represents the linear-plateau regression $y = \begin{cases} y_{max}, & REW > REW_{th} \\ aREW + b, & REW \leq REW_{th} \end{cases}$. Binned data are shown with the corresponding standard deviation (SD). The gray vertical lines indicate $REW_{th} \pm$ SD.

3.3 Limitation analysis

The first limitation analysis scheme used in this study consists in partitioning photosynthesis limitations under high irradiance between L_{gm}, L_{Vcmax}, and L_{gs} (Jones, 1985). L_{gs} was always higher than L_{gm} above REW ~ 0.28 (Figure 3A), where L_{gm} became predominant over L_{gs} (i.e., intersection of L_{gs} and L_{gm}; Figure 3B). When REW was minimum, 34% of the decrease in A_{sat} was explained by L_{gs}, 20% by L_{Vcmax}, and 56% by L_{gm} (Figures 3A, B).

This limitation scheme indicated that CO_2 diffusion factors (i.e., L_{gm} and L_{gs}) explained most of the decrease in A_{sat} with a similar contribution. However, using g_s in the partitioning analysis does not allow to fully identify the origin of the early stomatal closure, as g_s itself can be influenced by V_{cmax} and g_m through A_{sat} (Equation 8). This hypothesis is supported by the similar REW threshold for g_s and $g_{m,25}$, which suggests that the two variables are closely related. Combining Equations 16, 10 showed that the increase in L_{gs} is mostly caused by g_m and VPD notably under mild soil water conditions ($REW > REW_{th,CiCs}$, ; Figure 4). In particular, $L_{gm,USO}$

TABLE 1 Statistics of the segmented linear regression for the response of A_{sat}, $V_{cmax,25}$, g_s, $g_{m,25}$, g_1, C_i/C_s and to REW.

	A_{sat} (µmol m^{-2} s^{-1})	$V_{cmax,25}$ (µmol m^{-2} s^{-1})	g_s (mol m^{-2} s^{-1})	$g_{m,25}$ (mol m^{-2} s^{-1})	g_1 (kPa$^{0.5}$)	C_i/C_s (-)
$y = \begin{cases} y_{max}, & x > REW_{th} \\ ax + b, & x \le REW_{th} \end{cases}$						
Y_{max} (± SD)	18.74 ± 1.00	264.02 ± 11.63	0.10 ± 0.01	0.15 ± 0.01	1.39 ± 0.17	0.48 ± 0.02
α (± SD)	35.22 ± 8.38	1125.2 ± 387.6	0.18 ± 0.06	0.29 ± 0.11	−52.67 ± 9.83	−2.59 ± 1.12
b (± SD)	−6.73 ± 3.86	−255.2 ± 127.9	−0.03 ± 0.03	−0.06 ± 0.05	20.15 ± 3.06	1.43 ± 0.35
REW_{th} (± SD)	0.72 ± 0.08	0.43 ± 0.04	0.73 ± 0.12	0.72 ± 0.13	0.36 ± 0.01	0.37 ± 0.03
R^2	0.70	0.74	0.55	0.66	0.77	0.47

Parameters are given with their standard deviation (SD).
REW, relative extractable water.

was always higher than $L_{VPD,USO}$ and $L_{Vcmax,USO}$ (Figure 4). Moreover, g_1 had a positive contribution to L_{gs} (Figure 4), which indicates that the increase in g_1 (Figure 2E) promoted the opening of stomata to sustain CO_2 diffusion to the fixation sites. Once the USO model has been integrated in the limitation analysis on A_{sat}, it can be shown that $L_{gm,USO}$ was predominant over $L_{VPD,USO}$ regardless of soil water conditions (Figure 5A). When REW was minimum, 69% of the decrease in A_{sat} was explained by $L_{gm,USO}$, 31% by $L_{Vcmax,USO}$, and 20% by $L_{VPD,USO}$ (Figure 5A). In these conditions, $L_{g1,USO}$ was positive and reached 40%. The positive contribution of g_1 can be explained by the increase in dg_1/g_1 (Figure 2E), which resulted in an increase in $L_{g1,USO}$ (Equation 15). Such increase in $L_{g1,USO}$ was observed from $REW_{th,\ g1,CiCs}$ (Tables 1, 2), which corresponded to low A_{sat} (6.8 µmol m^{-2} s^{-1}) and g_s (0.04 mol m^{-2} s^{-1}). Note that the sum of all curves in Figure 5B may not necessarily equal 1, as the sum of limiting components when using the USO partitioning scheme did not exactly correspond to dA_{sat}/A_{sat} because of the uncertainties associated with the fitting of the linear-plateau segmented model on measurements (Figures 2, 5A).

4 Discussion

The determination of thresholds of soil water availability impacting CO_2 assimilation is pivotal for calibrating the response of photosynthesis model parameters during drying-up episodes (Vidale et al., 2021). The results of this study showed that soil water-limiting conditions induced a two-stage response of potato to water stress, with g_s and g_m being the first variables impacted by the decrease in REW followed by biochemical limitations through the decrease in V_{cmax}. In addition, we used a new partitioning scheme where the total derivative of g_s was written as a function of its explanatory variables in the USO model (i.e., g_1, V_{cmax}, VPD, and A_{sat}). This method allowed to quantify the origins of the decrease in A_{sat} in response to changes in g_m, V_{cmax}, g_1, and VPD. This partitioning was compared to the original formulation of photosynthesis limitations of Jones (1985), which attributed the origins of the reduction of A_{sat} to the relative variations of g_m, V_{cmax}, and g_s. The comparison between the two schemes provides an estimation of the importance of the factors influencing g_s and A_{sat}.

4.1 Predominance of CO_2 diffusion constraints on photosynthesis

Stomatal closure is a well-known mechanism of potato to reduce transpiration under water stress (Gerhards et al., 2016; Gordon et al., 1997; Obidiegwu, 2015; Romero et al., 2017; Vos and Oyarzún, 1987). Stomatal closure dynamics are complex and can be directly caused by the evaporation of the water held by guard cells or by the loss of turgor pressure induced by sensing of signaling molecules (Bharath et al., 2021; Ding and Chaumont, 2020; Obidiegwu, 2015; Pirasteh-Anosheh et al., 2016; Zhang et al., 2022). These mechanisms are likely

TABLE 2 p-Value of the t-test comparing REW_{th} between A_{sat}, V_{cmax25}, g_s, g_{m25}, g_1, and C_i/C_s.

p-Value REW_{th}	A_{sat}	$V_{cmax,25}$	g_s	$g_{m,25}$	g_1	C_i/C_s
A_{sat}	–					
$V_{cmax,25}$	0.000***	–				
g_s	0.89^{ns}	0.000***	–			
$g_{m,25}$	0.69^{ns}	0.000***	0.89^{ns}	–		
g_1	0.00***	0.000***	0.000***	0.000***	–	
C_i/C_s	0.00***	0.000***	0.000***	0.000***	0.05^{ns}	–

*** indicates when the p-value is <0.001 and ns when >0.05.

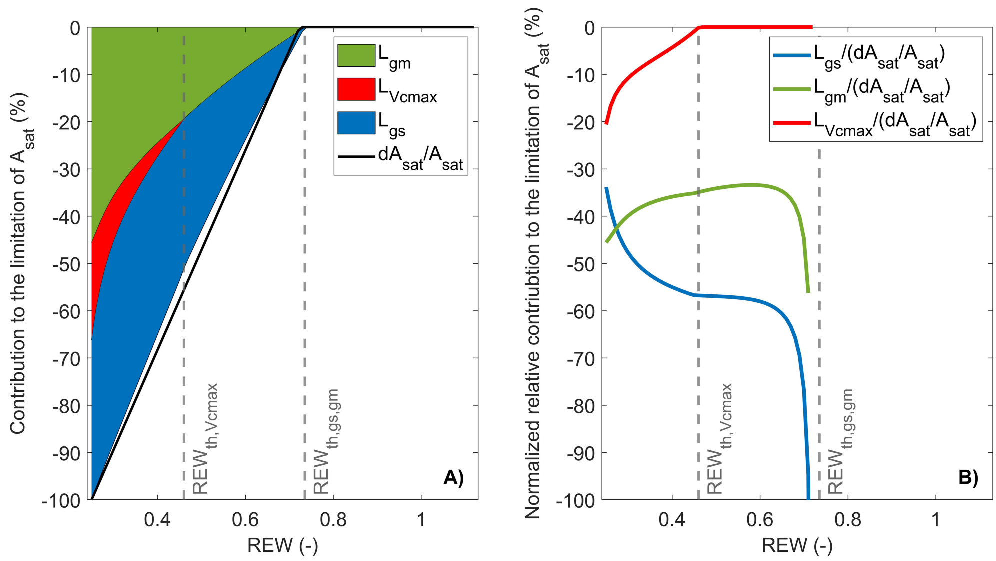

FIGURE 3
Partitioning of A_{sat} limitations between L_{gs}, L_{gm}, and L_{Vcmax} in response to relative extractable water (REW) with stacked limitation curves **(A)** and normalized relative contribution curves **(B)**. The black line is the relative variation of A_{sat} compared to its maximum value (i.e., y_{max} of the linear-plateau regression), and the gray vertical lines indicate REW_{th} ± SD.

to be synchronized with those influencing mesophyll conductance as evidenced by a similar REW threshold for g_s and g_m (Figure 2). In particular, mesophyll and stomatal conductance share similar responses to abscisic acid (Flexas et al., 2012; Li et al., 2021; Sorrentino et al., 2016), internal CO_2 concentration (Engineer et al., 2016; Tan et al., 2017), or starch-derived molecules (Lawson et al., 2014), which leads to similar responses under water stress (Flexas et al., 2004; Wang et al., 2018; Xiong et al., 2018). L_{gm} became predominant over L_{gs} under severe water stress, which was associated with a very low g_m and a strong restriction of CO_2 diffusion to chloroplasts (Figures 2, 3). While this partitioning scheme indicated that photosynthesis limitations mostly originated from g_s, it did not highlight the influence of non-stomatal factors on stomatal conductance. The origins of the decrease in g_s and A_{sat} can be identified using the USO model equation in the limitation analysis. In particular, the USO partitioning scheme showed that most stomatal

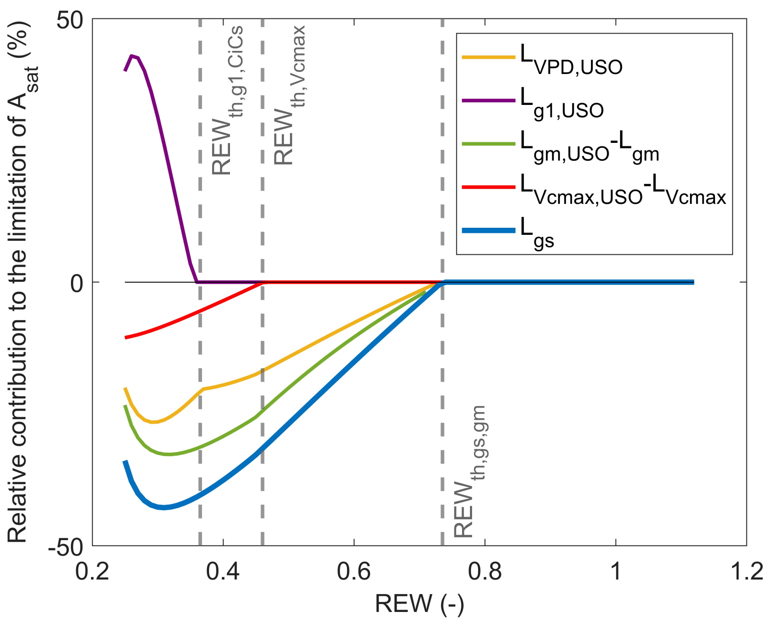

FIGURE 4
Partitioning of the limiting component induced by stomatal closure (L_{gs}) into $L_{g1,USO}$, $L_{gm,USO} - L_{gm}$, $L_{Vcmax,USO} - L_{Vcmax}$, and $L_{VPD,USO}$ in response to relative extractable water (REW). The gray vertical lines indicate REW_{th} ± SD.

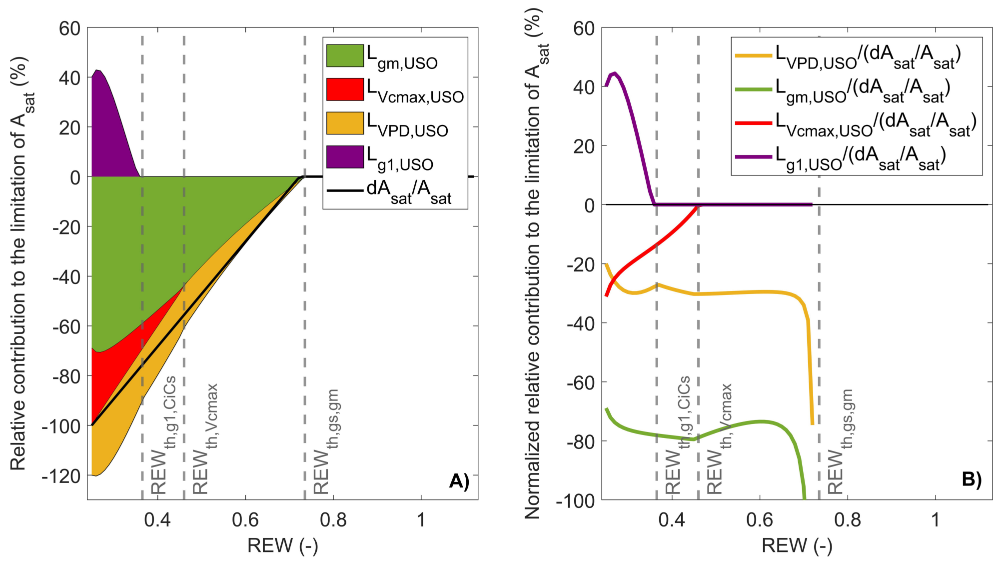

FIGURE 5
Partitioning of A_{sat} limitations between $L_{g1,USO}$, $L_{gm,USO}$, $L_{Vcmax,USO}$, and $L_{VPD,USO}$ in response to relative extractable water (REW) with stacked limitation curves **(A)** and shows normalized relative contribution curves **(B)**. The black line is the relative variation of A_{sat} compared to its maximum value (i.e., y_{max} of the linear-plateau regression), and the gray vertical lines indicate REW_{th} ± SD.

closure dynamics can be attributed to a combined effect of g_m and VPD (Figure 4). More specifically, $L_{gm,USO}$ was always higher than the other limiting components (Figures 5A, B), which highlights the strong control of mesophyll conductance on stomatal closure through its influence on A_{sat} regardless of REW values. These results confirm the importance of the mesophyll constraint for potato, as also highlighted in numerous species across PFTs (Cano et al., 2013; Flexas et al., 2009; Galmés et al., 2007; Grassi and Magnani, 2005; Limousin et al., 2010; Perez-Martin et al., 2014; Wang et al., 2018; Wang et al., 2018; Zait and Schwartz, 2018; Zhu et al., 2021) and emphasize the importance of including the effect of REW on g_m in LSMs (Knauer et al., 2020). This study also provides a calibration of the water stress factor for potato and contributes to reducing the uncertainties when estimating carbon assimilation and transpiration under water stress (Vidale et al., 2021). Additional information on the description of the physiological effects of mesophyll on stomatal closure can be found in Lemonnier and Lawson (2023). Since disentangling the primary metabolisms that synchronously control photosynthesis, stomatal, and mesophyll conductance remains challenging, future studies would benefit from additional molecular or anatomical measurements to unravel the interplays between stomatal and non-stomatal factors (Gago et al., 2020).

4.2 Relationship between photosynthesis and stomatal conductance under severe drought

Severe restrictions in soil water availability induced a decrease in V_{cmax} as well as an increase in g_1 and C_i/C_s (Figure 2). An increase in C_i/C_s can be observed under strong limitations in CO_2 diffusion and decreasing photosynthetic activity (Bermúdez-Cardona et al., 2015; Brodribb, 1996; Huang, 2020; Tan et al., 2017). In particular, C_i/C_s increased when g_s was lower than 0.04 mol m^{-2} s^{-1}, which was already reported as a stomatal conductance threshold for such C_i-inflexion point in various species (Blankenagel et al., 2018; Brodribb, 1996; Flexas, 2002; Martin and Ruiz-Torres, 1992; Rouhi et al., 2007) including potato (Ramírez et al., 2016). In these conditions of photosynthesis inhibition, the excess energy carried by sun irradiance must be metabolized by alternative processes such as xanthophyll (Demmig-Adams et al., 2012), lutein (García-Plazaola et al., 2003), and photorespiratory cycles (Osmond et al., 1980). This last may contribute to the increase in C_i/C_s by emitting CO_2 through the glycine decarboxylase enzyme (Busch et al., 2017; Shi and Bloom, 2021).

The increase in g_1 induced an increase in dg_1/g_1 and L_{g1} when $REW < REW_{th,g1,CiCs}$ (Figures 2, 4A, B). g_1 is inversely related to the marginal carbon cost of water, which corresponds to the change in carbon gained per unit of water transpired, also known as marginal WUE (Medlyn et al., 2011). The increase in g_1 can be explained by either i) an increase in transpiration per unit of carbon gained by photosynthesis or ii) a decrease in photosynthesis per unit of water transpired (Medlyn et al., 2011). For example, increasing stomatal conductance to promote transpiration may help in cooling down leaf surfaces during heatwaves at the expense of increasing mortality risks through hydraulic vulnerability and cavitation (Marchin et al., 2022; Urban et al., 2017). Numerous studies have highlighted such cooling effect on potato (Sprenger et al., 2016; Zhang et al., 2022), which can ultimately lead to an increase in g_1 (Marchin et al., 2023). A decoupling between stomatal conductance and photosynthesis may be the consequence of an adaptive strategy (i.e., sacrificing water for leaf survival and future carbon gains) or the increasing viscosity of water at high temperatures, which facilitates the transport of water in the vascular system (Marchin et al., 2023). In our experiment, the lowest measurement of g_s was 0.011 mol m^{-2} s^{-1}, which is higher than the reported value of minimum stomatal conductance for CO_2 transfer across plant species (i.e., g_s = 0.008 mol m^{-2} s^{-1}; Duursma et al., 2019) and suggests that stomata may not be fully closed. It is, however, unlikely that potato plants had access to water to sustain transpiration through stomata or cuticles because of the low REW values that were observed in these conditions (Figure 2). Alternatively, the increase in g_1 may be caused by a decrease in photosynthesis through the additional effect of NSOL on A_{sat} (Beauclaire et al., 2023; Gourlez de la Motte et al., 2020), which intensifies the decoupling between carbon assimilation and stomatal conductance by decreasing WUE (Manzoni et al., 2011). This hypothesis is supported by previous studies, which have shown that irrigation enhances WUE for potato (Akkamis and Caliskan, 2023; Ati et al., 2012).

The increase in g_1 induced a positive contribution to dA_{sat}/A_{sat} (Figure 5), suggesting that potato plants promoted the loss of water to the benefit of CO_2 diffusion despite the risks for the hydraulic and photosynthetic systems when carbon assimilation reached critical levels under drought (Deva et al., 2020; Reynolds-Henne et al., 2010). It indicates a shift in the optimal balance point between carbon gain and water loss where potato plants are willing to lose more water per unit of carbon gained (Zhou et al., 2013). This prioritization is not likely to be driven by optimizing survival under severe drought conditions where soil water is hardly accessible and hydraulic limitations presumably important. Instead, the increase in g_1 could be interpreted as a deviation from optimal stomatal behavior. The stomatal optimality theory states that any increase in the plant's carbon gain should equal the evaporative water loss proportionally to the carbon cost of water (Cowan and Farquhar, 1977). The optimality theory holds under the assumption that the curvature of photosynthesis versus transpiration is negative; that is, increments of A tend to become smaller with increments of g_s, as stomata reduce the gradient for CO_2 uptake more than that for H_2O loss (Buckley et al., 2017). Any conditions shifting the curve to a positive curvature will cause a deviation from the optimality theory, challenging the interpretation of g_1 short-term dynamics. Two of these conditions were likely observed in this study: first, an additional restriction of CO_2 diffusion to chloroplasts by mesophyll conductance and, second, a possible hydraulic impairment at very low REW, which ultimately changes the photosynthesis–transpiration relationship (Buckley et al., 2017; Cowan and Farquhar, 1977). This unrealistic stomatal opening response is consistent with previous studies that have shown a similar increase in g_1 under severe drought (Beauclaire et al., 2023; Gourlez de la Motte et al., 2020; Zhou et al., 2013), arguing for a refinement of stomatal optimality. Novel modeling approaches consider the cost of stomatal opening as a function of an increase in NSOL (Dewar et al., 2018), or hydraulic impairment using profit maximization optimization (Sperry et al., 2017) may be preferred to interpret stomatal dynamics under drought conditions.

4.3 Methodological considerations

g_m was determined by the "variable J" method at light saturation (Harley et al., 1992), which is sensitive to variation in R_d and Γ^* (Pons et al., 2009; Théroux-Rancourt et al., 2014). These two variables can be impacted by drought and heat stress, which was not considered in the method part. First, it has been shown that R_d can increase under water stress due to the additional release of CO_2 from mitochondria by the photorespiratory cycle (Busch et al., 2017; Pinheiro and Chaves, 2011). Second, the sensitivity of Γ^* to temperature can change under critical levels (usually above 30°C), which may invalidate the parameterization on leaf temperature (Bernacchi et al., 2001). Measuring the CO_2 compensation point (Walker and Ort, 2015) and leaf respiration (Yin and Amthor, 2024) under drought could help resolve these uncertainties.

The diffusion of water vapor through the cuticle and epidermis may become significant compared to stomatal diffusion under water stress (Boyer, 2015a; Boyer, 2015b; Boyer et al., 1997). As the transpiration flux measured by gas exchange measurement systems corresponds to the sum of the diffusion through stomatal and cuticle conductance, C_i overestimations can occur as the Fick law considers an identical gas phase path for CO_2 and H_2O. Direct measurements of C_i by a modified gas exchange device (Boyer and Kawamitsu, 2011) or a modification of the Fick law by quantifying the cuticle conductance (Wang et al., 2018) could increase the accuracy of C_i under water stress.

Lastly, none of the current methods for estimating g_m actually measure diffusion plant conductance. This paper interprets g_m as an internal diffusion plant conductance limiting CO_2 diffusion from substomatal cavities to carboxylation sites in the chloroplasts. This two-dimensional view of CO_2 diffusion is a simplification of the actual pathway where sink and sources are distributed along the way. The widely adopted definition of mesophyll conductance (i.e., $A/(C_i - C_c)$) simplifies the leaf as a single sink and ignores the complexity of the mesophyll structure, as well as the heterogeneity in photosynthetic capacities and cellular structure of the leaf vertical light absorption profile (Evans et al., 2009). A more realistic view of mesophyll conductance should include i) a decomposition of resistive components on the CO_2 pathway such as cell wall and membrane, cytosol, chloroplast envelope, and stroma resistances (Cousins et al., 2020); ii) three-dimensional modeling across the leaf vertical profile (Théroux-Rancourt and Gilbert, 2017; Xiao and Zhu, 2017); and iii) a quantification of chloroplast movement, which is a key driver of g_m (Carriquí et al., 2019) and is sensitive to changes in light absorption peaks (Tholen et al., 2008). However, most of the complexity can be, neglected when measurements are conducted at light saturation (Théroux-Rancourt and Gilbert, 2017). Improvements in the techniques for estimating the contribution of the different resistive components would help in understanding the response of g_m to anatomical and biochemical drivers under drought (Evans, 2021).

Data availability statement

The raw data supporting the conclusions of this article will be made available by the authors, without undue reservation.

Author contributions

QB: Writing – original draft, Visualization, Resources, Methodology, Investigation, Formal analysis, Conceptualization. FV: Writing – review & editing, Resources, Investigation. BL: Writing – review & editing, Supervision, Project administration, Methodology, Formal analysis, Conceptualization.

Funding

The author(s) declare financial support was received for the research, authorship, and/or publication of this article. The researchers were funded by the Fédération Wallonie-Bruxelles.

Acknowledgments

This study was conducted with the support of the research and teaching support units “Environment Is Life” and “Agriculture Is Life” of Gembloux Agro-Bio Tech, University of Liege, Belgium.

Conflict of interest

The authors declare that the research was conducted in the absence of any commercial or financial relationships that could be construed as a potential conflict of interest.

Publisher’s note

Supplementary material

The Supplementary Material for this article can be found online at: https://www.frontiersin.org/articles/10.3389/fpls.2024.1500624/full#supplementary-material

References

Akkamis, M., and Caliskan, S. (2023). Responses of yield, quality and water use efficiency of potato grown under different drip irrigation and nitrogen levels. *Sci. Rep.* 13, 9911. doi: 10.1038/s41598-023-36934-3

Anderegg, W. R. L., Trugman, A. T., Bowling, D. R., Salvucci, G., and Tuttle, S. E. (2019). Plant functional traits and climate influence drought intensification and land–atmosphere feedbacks. *Proc. Natl. Acad. Sci. U.S.A.* 116, 14071–14076. doi: 10.1073/pnas.1904747116

Archontoulis, S. V., and Miguez, F. E. (2015). Nonlinear regression models and applications in agricultural research. *Agron. J.* 107, 786–798. doi: 10.2134/agronj2012.0506

Ati, A. S., Iyada, A. D., and Najim, S. M. (2012). Water use efficiency of potato (Solanum tuberosum L.) under different irrigation methods and potassium fertilizer rates. *Ann. Agric. Sci.* 57, 99–103. doi: 10.1016/j.aoas.2012.08.002

Beauclaire, Q., Heinesch, B., and Longdoz, B. (2023). Non-stomatal processes are responsible for the decrease in gross primary production of a potato crop during edaphic drought. *Agric. For. Meteorology* 343, 109782. doi: 10.1016/j.agrformet.2023.109782

Bermúdez-Cardona, M. B., Filho, J. A. W., and Rodrigues, F.Á. (2015). Leaf gas exchange and chlorophyll a fluorescence in maize leaves infected with *Stenocarpella macrospora*. *Phytopathology®* 105, 26–34. doi: 10.1094/PHYTO-04-14-0096-R

Bernacchi, C. J., Portis, A. R., Nakano, H., von Caemmerer, S., and Long, S. P. (2002). Temperature response of mesophyll conductance. Implications for the determination of Rubisco enzyme kinetics and for limitations to photosynthesis in vivo. *Plant Physiol.* 130, 1992–1998. doi: 10.1104/pp.008250

Bernacchi, C. J., Singsaas, E. L., Pimentel, C., Portis, J. A. R., and Long, S. P. (2001). Improved temperature response functions for models of Rubisco-limited photosynthesis: *In vivo* Rubisco enzyme kinetics. *Plant Cell Environ.* 24, 253–259. doi: 10.1111/j.1365-3040.2001.00668.x

Bertolino, L. T., Caine, R. S., and Gray, J. E. (2019). Impact of stomatal density and morphology on water-use efficiency in a changing world. *Front. Plant Sci.* 10. doi: 10.3389/fpls.2019.00225

Bharath, P., Gahir, S., and Raghavendra, A. S. (2021). Abscisic acid-induced stomatal closure: an important component of plant defense against abiotic and biotic stress. *Front. Plant Sci.* 12. doi: 10.3389/fpls.2021.615114

Blankenagel, S., Yang, Z., Avramova, V., Schön, C.-C., and Grill, E. (2018). Generating plants with improved water use efficiency. *Agronomy* 8, 194. doi: 10.3390/agronomy8090194

Boyer, J. S. (2015a). Turgor and the transport of CO2 and water across the cuticle (epidermis) of leaves. *J. Exp. Bot.* 66, 2625–2633. doi: 10.1093/jxb/erv065

Boyer, J. S. (2015b). Impact of cuticle on calculations of the CO2 concentration inside leaves. *Planta* 242, 1405–1412. doi: 10.1007/s00425-015-2378-1

Boyer, J. S., and Kawamitsu, Y. (2011). Photosynthesis gas exchange system with internal CO2 directly measured. *Environ. Control Biol.* 49, 193–207. doi: 10.2525/ecb.49.193

Boyer, J. S., Wong, S. C., and Farquhar, G. D. (1997). CO2 and Water Vapor Exchange across Leaf Cuticle (Epidermis) at Various Water Potentials. *Plant Physiol.* 114, 185–191. doi: 10.1104/pp.114.1.185

Brodribb, T. (1996). Dynamics of Changing Intercellular CO2 Concentration (ci) during Drought and Determination of Minimum Functional ci. *Plant Physiol.* 111, 179–185. doi: 10.1104/pp.111.1.179

Buckley, T. N., Sack, L., and Farquhar, G. D. (2017). Optimal plant water economy. *Plant Cell Environ.* 40, 881–896. doi: 10.1111/pce.12823

Burnham, K. P., Anderson, D. R., and Burnham, K. P. (2002). *Model selection and multimodel inference: a practical information-theoretic approach, 2nd ed. ed* (New York: Springer).

Burnham, K. P., Anderson, D. R., and Huyvaert, K. P. (2011). AIC model selection and multimodel inference in behavioral ecology: some background, observations, and comparisons. *Behav. Ecol. Sociobiol* 65, 23–35. doi: 10.1007/s00265-010-1029-6

Busch, F. A., Deans, R. M., and Holloway-Phillips, M.-M. (2017). “Estimation of photorespiratory fluxes by gas exchange,” in *Photorespiration, Methods in Molecular Biology*. Eds. A. R. Fernie, H. Bauwe and A. P. M. Weber (Springer New York, New York, NY), 1–15. doi: 10.1007/978-1-4939-7225-8_1

Cano, F. J., Sánchez-Gómez, D., Rodríguez-Calcerrada, J., Warren, C. R., Gil, L., and Aranda, I. (2013). Effects of drought on mesophyll conductance and photosynthetic limitations at different tree canopy layers: Limitations to carbon uptake into the canopy. *Plant Cell Environ*. doi: 10.1111/pce.12103

Carriquí, M., Roig-Oliver, M., Brodribb, T. J., Coopman, R., Gill, W., Mark, K., et al. (2019). Anatomical constraints to nonstomatal diffusion conductance and photosynthesis in lycophytes and bryophytes. *New Phytol.* 222, 1256–1270. doi: 10.1111/nph.15675

Chang, H., and Bonnette, M. R. (2016). Climate change and water-related ecosystem services: impacts of drought in California, USA. *Ecosyst. Health Sustain* 2, e01254. doi: 10.1002/ehs2.1254

Clogg, C. C., Petkova, E., and Haritou, A. (1995). Statistical methods for comparing regression coefficients between models. *Am. J. Sociology* 100, 1261–1293. doi: 10.1086/230638

Cousins, A. B., Mullendore, D. L., and Sonawane, B. V. (2020). Recent developments in mesophyll conductance in C3, C4, and crassulacean acid metabolism plants. *Plant J.* 101, 816–830. doi: 10.1111/tpj.14664

Cowan, I., and Farquhar, G. (1977). Stomatal function in relation to leaf metabolism and environment. *Symp. Soc. Exp. Biol.* 31, 471—505.

De Kauwe, M. G., Lin, Y.-S., Wright, I. J., Medlyn, B. E., Crous, K. Y., Ellsworth, D. S., et al. (2016). A test of the 'one-point method' for estimating maximum carboxylation capacity from field-measured, light-saturated photosynthesis. *New Phytol.* 210, 1130–1144. doi: 10.1111/nph.13815

Demmig-Adams, B., Cohu, C. M., Muller, O., and Adams, W. W. (2012). Modulation of photosynthetic energy conversion efficiency in nature: from seconds to seasons. *Photosynth Res.* 113, 75–88. doi: 10.1007/s11120-012-9761-6

Deva, C. R., Urban, M. O., Challinor, A. J., Falloon, P., and Svitákova, L. (2020). Enhanced leaf cooling is a pathway to heat tolerance in common bean. *Front. Plant Sci.* 11. doi: 10.3389/fpls.2020.00019

Dewar, R., Mauranen, A., Mäkelä, A., Hölttä, T., Medlyn, B., and Vesala, T. (2018). New insights into the covariation of stomatal, mesophyll and hydraulic conductances from optimization models incorporating nonstomatal limitations to photosynthesis. *New Phytol.* 217, 571–585. doi: 10.1111/nph.14848

Ding, L., and Chaumont, F. (2020). Are aquaporins expressed in stomatal complexes promising targets to enhance stomatal dynamics? *Front. Plant Sci.* 11. doi: 10.3389/fpls.2020.00458

Duursma, R. A., Blackman, C. J., Lopéz, R., Martin-StPaul, N. K., Cochard, H., and Medlyn, B. E. (2019). On the minimum leaf conductance: its role in models of plant water use, and ecological and environmental controls. *New Phytol.* 221, 693–705. doi: 10.1111/nph.15395

Engineer, C. B., Hashimoto-Sugimoto, M., Negi, J., Israelsson-Nordström, M., Azoulay-Shemer, T., Rappel, W.-J., et al. (2016). CO2 sensing and CO2 regulation of stomatal conductance: advances and open questions. *Trends Plant Sci.* 21, 16–30. doi: 10.1016/j.tplants.2015.08.014

Evans, J. R. (2021). Mesophyll conductance: walls, membranes and spatial complexity. *New Phytol.* 229, 1864–1876. doi: 10.1111/nph.16968

Evans, J. R., Kaldenhoff, R., Genty, B., and Terashima, I. (2009). Resistances along the CO2 diffusion pathway inside leaves. *J. Exp. Bot.* 60, 2235–2248. doi: 10.1093/jxb/erp117

Fahad, S., Bajwa, A. A., Nazir, U., Anjum, S. A., Farooq, A., Zohaib, A., et al. (2017). Crop production under drought and heat stress: plant responses and management options. *Front. Plant Sci.* 8. doi: 10.3389/fpls.2017.01147

Farquhar, G. D., and Sharkey, T. D. (1982). Stomatal conductance and photosynthesis. *Annu. Rev. Plant Physiol.* 33, 317–345. doi: 10.1146/annurev.pp.33.060182.001533

Farquhar, G. D., von Caemmerer, S., and Berry, J. A. (1980). A biochemical model of photosynthetic CO2 assimilation in leaves of C3 species. *Planta* 149, 78–90. doi: 10.1007/BF00386231

Flexas, J. (2002). Drought-inhibition of photosynthesis in C3 plants: stomatal and non-stomatal limitations revisited. *Ann. Bot.* 89, 183–189. doi: 10.1093/aob/mcf027

Flexas, J., Barbour, M. M., Brendel, O., Cabrera, H. M., Carriquí, M., Díaz-Espejo, A., et al. (2012). Mesophyll diffusion conductance to CO2: An unappreciated central player in photosynthesis. *Plant Sci.* 193–194, 70–84. doi: 10.1016/j.plantsci.2012.05.009

Flexas, J., Barón, M., Bota, J., Ducruet, J.-M., Gallé, A., Galmés, J., et al. (2009). Photosynthesis limitations during water stress acclimation and recovery in the drought-adapted Vitis hybrid Richter-110 (V. *berlandieri×V. rupestris). J. Exp. Bot.* 60, 2361–2377. doi: 10.1093/jxb/erp069

Flexas, J., Bota, J., Loreto, F., Cornic, G., and Sharkey, T. D. (2004). Diffusive and metabolic limitations to photosynthesis under drought and salinity in C_3 plants. *Plant Biol.* 6, 269–279. doi: 10.1055/s-2004-820867

Gago, J., Daloso, D. M., Carriquí, M., Nadal, M., Morales, M., Araújo, W. L., et al. (2020). Mesophyll conductance: the leaf corridors for photosynthesis. *Biochem. Soc. Trans.* 48, 429–439. doi: 10.1042/BST20190312

Galmés, J., Medrano, H., and Flexas, J. (2007). Photosynthetic limitations in response to water stress and recovery in Mediterranean plants with different growth forms. *New Phytol.* 175, 81–93. doi: 10.1111/j.1469-8137.2007.02087.x

García-Plazaola, J. I., Hernández, A., Olano, J. M., and Becerril, J. M. (2003). The operation of the lutein epoxide cycle correlates with energy dissipation. *Funct. Plant Biol.* 30, 319. doi: 10.1071/FP02224

Genty, B., Briantais, J.-M., and Baker, N. R. (1989). The relationship between the quantum yield of photosynthetic electron transport and quenching of chlorophyll fluorescence. *Biochim. Biophys. Acta (BBA) - Gen. Subj.* 990, 87–92. doi: 10.1016/S0304-4165(89)80016-9

Gerhards, M., Rock, G., Schlerf, M., and Udelhoven, T. (2016). Water stress detection in potato plants using leaf temperature, emissivity, and reflectance. *Int. J. Appl. Earth Observation Geoinformation* 53, 27–39. doi: 10.1016/j.jag.2016.08.004

Gervais, T., Creelman, A., Li, X.-Q., Bizimungu, B., De Koeyer, D., and Dahal, K. (2021). Potato response to drought stress: physiological and growth basis. *Front. Plant Sci.* 12. doi: 10.3389/fpls.2021.698060

Goffart, J.-P., Haverkort, A., Storey, M., Haase, N., Martin, M., Lebrun, P., et al. (2022). Potato production in northwestern europe (Germany, France, the Netherlands, United Kingdom, Belgium): characteristics, issues, challenges and opportunities. *Potato Res.* doi: 10.1007/s11540-021-09535-8

Gordon, R., Brown, D. M., and Dixon, M. A. (1997). Estimating potato leaf area index for specific cultivars. *Potato Res.* 40, 251–266. doi: 10.1007/BF02358007

Gourlez de la Motte, L., Beauclaire, Q., Heinesch, B., Cuntz, M., Foltýnová, L., Sigut, L., et al. (2020). Non-stomatal processes reduce gross primary productivity in temperate forest ecosystems during severe edaphic drought. *Philos. Trans. R. Soc. B Biol. Sci. In Press.* doi: 10.1098/RSTB-2019-0527

Granier, A., Reichstein, M., Bréda, N., Janssens, I. A., Falge, E., Ciais, P., et al. (2007). Evidence for soil water control on carbon and water dynamics in European forests during the extremely dry year: 2003. *Agric. For. Meteorology* 143, 123–145. doi: 10.1016/j.agrformet.2006.12.004

Grassi, G., and Magnani, F. (2005). Stomatal, mesophyll conductance and biochemical limitations to photosynthesis as affected by drought and leaf ontogeny in ash and oak trees. *Plant Cell Environ.* 28, 834–849. doi: 10.1111/j.1365-3040.2005.01333.x

Harley, P. C., Loreto, F., Di Marco, G., and Sharkey, T. D. (1992). Theoretical considerations when estimating the mesophyll conductance to CO_2 flux by analysis of the response of photosynthesis to CO_2. *Plant Physiol.* 98, 1429–1436. doi: 10.1104/pp.98.4.1429

Hartick, C., Furusho-Percot, C., Clark, M. P., and Kollet, S. (2022). An interannual drought feedback loop affects the surface energy balance and cloud properties. *Geophysical Res. Lett.* 49, e2022GL100924. doi: 10.1029/2022GL100924

Hendrawan, V. S. A., Kim, W., Touge, Y., Ke, S., and Komori, D. (2022). A global-scale relationship between crop yield anomaly and multiscalar drought index based on multiple precipitation data. *Environ. Res. Lett.* 17, 014037. doi: 10.1088/1748-9326/ac45b4

Héroult, A., Lin, Y.-S., Bourne, A., Medlyn, B. E., and Ellsworth, D. S. (2013). Optimal stomatal conductance in relation to photosynthesis in climatically contrasting *Eucalyptus* species under drought: Stomatal responses of eucalyptus under drought. *Plant Cell Environ.* 36, 262–274. doi: 10.1111/j.1365-3040.2012.02570.x

Huang, Z. (2020). Soil water availability threshold indicator was determined by using plant physiological responses under drought conditions. *Ecol. Indic.* 10. doi: 10.1016/j.ecolind.2020.106740

Jones, H. G. (1985). Partitioning stomatal and non-stomatal limitations to photosynthesis. *Plant Cell Environ.* 8, 95–104. doi: 10.1111/j.1365-3040.1985.tb01227.x

Kala, J., De Kauwe, M. G., Pitman, A. J., Lorenz, R., Medlyn, B. E., Wang, Y.-P., et al. (2015). Implementation of an optimal stomatal conductance scheme in the Australian Community Climate Earth Systems Simulator (ACCESS1.3b). *Geosci. Model. Dev.* 8, 3877–3889. doi: 10.5194/gmd-8-3877-2015

Kang, H., Sridhar, V., Mainuddin, M., and Trung, L. D. (2021). Future rice farming threatened by drought in the Lower Mekong Basin. *Sci. Rep.* 11, 9383. doi: 10.1038/s41598-021-88405-2

Knauer, J., El-Madany, T. S., Zaehle, S., and Migliavacca, M. (2018). Bigleaf—An R package for the calculation of physical and physiological ecosystem properties from eddy covariance data. *PloS One* 13, e0201114. doi: 10.1371/journal.pone.0201114

Knauer, J., Zaehle, S., De Kauwe, M. G., Haverd, V., Reichstein, M., and Sun, Y. (2020). Mesophyll conductance in land surface models: effects on photosynthesis and transpiration. *Plant J.* 101, 858–873. doi: 10.1111/tpj.14587

Kramer, D. M., Johnson, G., Kiirats, O., and Edwards, G. E. (2004). New fluorescence parameters for the determination of Q_A redox state and excitation energy fluxes. *Photosynthesis Res.* 79, 209–218. doi: 10.1023/B:PRES.0000015391.99477.0d

Lamour, J., Davidson, K. J., Ely, K. S., Le Moguédec, G., Leakey, A. D. B., Li, Q., et al. (2022). An improved representation of the relationship between photosynthesis and stomatal conductance leads to more stable estimation of conductance parameters and improves the goodness-of-fit across diverse data sets. *Global Change Biol.* 28, 3537–3556. doi: 10.1111/gcb.16103

Lawrence, D. M., Fisher, R. A., Koven, C. D., Oleson, K. W., Swenson, S. C., Bonan, G., et al. (2019). The community land model version 5: description of new features, benchmarking, and impact of forcing uncertainty. *J. Adv. Model. Earth Syst.* 11, 4245–4287. doi: 10.1029/2018MS001583

Lawson, T., Simkin, A. J., Kelly, G., and Granot, D. (2014). Mesophyll photosynthesis and guard cell metabolism impacts on stomatal behaviour. *New Phytol.* 203, 1064–1081. doi: 10.1111/nph.12945

Lemonnier, P., and Lawson, T. (2023). Calvin cycle and guard cell metabolism impact stomatal function. *Semin. Cell Dev. Biol.*, S1084952123000502. doi: 10.1016/j.semcdb.2023.03.001

Li, S., Liu, J., Liu, H., Qiu, R., Gao, Y., and Duan, A. (2021). Role of hydraulic signal and ABA in decrease of leaf stomatal and mesophyll conductance in soil drought-stressed tomato. *Front. Plant Sci.* 12. doi: 10.3389/fpls.2021.653186

Limousin, J.-M., Misson, L., Lavoir, A.-V., Martin, N. K., and Rambal, S. (2010). Do photosynthetic limitations of evergreen *Quercus ilex* leaves change with long-term increased drought severity? *Plant Cell Environ*. doi: 10.1111/j.1365-3040.2009.02112.x

Lupo, Y., and Moshelion, M. (2024). The balance of survival: Comparative drought response in wild and domesticated tomatoes. *Plant Sci.* 339, 111928. doi: 10.1016/j.plantsci.2023.111928

Lutaladio, N., and Castaldi, L. (2009). Potato: The hidden treasure. *J. Food Composition Anal.* 22, 491–493. doi: 10.1016/j.jfca.2009.05.002

Manzoni, S., Vico, G., Katul, G., Fay, P. A., Polley, W., Palmroth, S., et al. (2011). Optimizing stomatal conductance for maximum carbon gain under water stress: a meta-analysis across plant functional types and climates: Optimal leaf gas exchange under water stress. *Funct. Ecol.* 25, 456–467. doi: 10.1111/j.1365-2435.2010.01822.x

Marchin, R. M., Backes, D., Ossola, A., Leishman, M. R., Tjoelker, M. G., and Ellsworth, D. S. (2022). Extreme heat increases stomatal conductance and drought-induced mortality risk in vulnerable plant species. *Global Change Biol.* 28, 1133–1146. doi: 10.1111/gcb.15976

Marchin, R. M., Medlyn, B. E., Tjoelker, M. G., and Ellsworth, D. S. (2023). Decoupling between stomatal conductance and photosynthesis occurs under extreme heat in broadleaf tree species regardless of water access. *Global Change Biol.* 29, 6319–6335. doi: 10.1111/gcb.16929

Martin, B., and Ruiz-Torres, N. A. (1992). Effects of water-deficit stress on photosynthesis, its components and component limitations, and on water use efficiency in wheat (*Triticum aestivum* L.). *Plant Physiol.* 100, 733–739. doi: 10.1104/pp.100.2.733

Martínez-Vilalta, J., Poyatos, R., Aguadé, D., Retana, J., and Mencuccini, M. (2014). A new look at water transport regulation in plants. *New Phytol.* 204, 105–115. doi: 10.1111/nph.12912

McAdam, S. A. M., and Brodribb, T. J. (2016). Linking turgor with ABA biosynthesis: implications for stomatal responses to vapor pressure deficit across land plants. *Plant Physiol.* 171, 2008–2016. doi: 10.1104/pp.16.00380

Medlyn, B. E., De Kauwe, M. G., Lin, Y.-S., Knauer, J., Duursma, R. A., Williams, C. A., et al. (2017). How do leaf and ecosystem measures of water-use efficiency compare? *New Phytol.* 216, 758–770. doi: 10.1111/nph.14626

Medlyn, B. E., Duursma, R. A., Eamus, D., Ellsworth, D. S., Prentice, I. C., Barton, C. V. M., et al. (2011). Reconciling the optimal and empirical approaches to modelling stomatal conductance: RECONCILING OPTIMAL AND EMPIRICAL STOMATAL MODELS. *Global Change Biol.* 17, 2134–2144. doi: 10.1111/j.1365-2486.2010.02375.x

Miao, Z., Xu, M., Lathrop, R. G., and Wang, Y. (2009). Comparison of the *A-C* $_c$ curve fitting methods in determining maximum ribulose 1·5-bisphosphate carboxylase/oxygenase carboxylation rate, potential light saturated electron transport rate and leaf dark respiration. *Plant Cell Environ.* 32, 109–122. doi: 10.1111/j.1365-3040.2008.01900.x

Miguez, F. (2023). *nlraa: Nonlinear regression for agricultural applications. (R PackageVersion 1.9.7)*. Available at: https://CRAN.R-project.org/package=nlraa.

Mrad, A., Sevanto, S., Domec, J.-C., Liu, Y., Nakad, M., and Katul, G. (2019). A dynamic optimality principle for water use strategies explains isohydric to anisohydric plant responses to drought. *Front. For. Glob. Change* 2. doi: 10.3389/ffgc.2019.00049

Nadal, M., and Flexas, J. (2018). "M esophyll C onductance to CO 2 D iffusion : E ffects of D rought and O pportunities for I mprovement," in *Water Scarcity and Sustainable Agriculture in Semiarid Environment* (Elsevier), 403–438. doi: 10.1016/B978-0-12-813164-0.00017-X

Nguyen, T. B.-A., Lefoulon, C., Nguyen, T.-H., Blatt, M. R., and Carroll, W. (2023). Engineering stomata for enhanced carbon capture and water-use efficiency. *Trends Plant Sci.* 28, 1290–1309. doi: 10.1016/j.tplants.2023.06.002

Niinemets, Ü., Cescatti, A., Rodeghiero, M., and Tosens, T. (2006). Complex adjustments of photosynthetic potentials and internal diffusion conductance to current and previous light availabilities and leaf age in Mediterranean evergreen species *Quercus ilex*. *Plant Cell Environ.* 29, 1159–1178. doi: 10.1111/j.1365-3040.2006.01499.x

Obidiegwu, J. E. (2015). Coping with drought: stress and adaptive responses in potato and perspectives for improvement. *Front. Plant Sci.* 6. doi: 10.3389/fpls.2015.00542

Osmond, C. B., Björkman, O., and Anderson, D. J. (1980). "Physiological processes in plant ecology: the structure for a synthesis," in *Physiological Processes in Plant Ecology: Toward a Synthesis with Atriplex*. Eds. C. B. Osmond, O. Björkman and D. J. Anderson (Springer Berlin Heidelberg, Berlin, Heidelberg), 1–11. doi: 10.1007/978-3-642-67637-6_1

Paternoster, R., Brame, R., Mazerolle, P., and Piquero, A. (1998). USING THE CORRECT STATISTICAL TEST FOR THE EQUALITY OF REGRESSION COEFFICIENTS. *Criminology* 36, 859–866. doi: 10.1111/j.1745-9125.1998.tb01268.x

Perez-Martin, A., Michelazzo, C., Torres-Ruiz, J. M., Flexas, J., Fernández, J. E., Sebastiani, L., et al. (2014). Regulation of photosynthesis and stomatal and mesophyll conductance under water stress and recovery in olive trees: correlation with gene expression of carbonic anhydrase and aquaporins. *J. Exp. Bot.* 65, 3143–3156. doi: 10.1093/jxb/eru160

Peters, W., van der Velde, I. R., van Schaik, E., Miller, J. B., Ciais, P., Duarte, H. F., et al. (2018). Increased water-use efficiency and reduced CO2 uptake by plants during droughts at a continental scale. *Nat. Geosci* 11, 744–748. doi: 10.1038/s41561-018-0212-7

Pinheiro, C., and Chaves, M. M. (2011). Photosynthesis and drought: can we make metabolic connections from available data? *J. Exp. Bot.* 62, 869–882. doi: 10.1093/jxb/erq340

Pirasteh-Anosheh, H., Saed-Moucheshi, A., Pakniyat, H., and Pessarakli, M. (2016). "Stomatal responses to drought stress," in *Water Stress and Crop Plants*. Ed. P. Ahmad (John Wiley & Sons, Ltd, Chichester, UK), 24–40. doi: 10.1002/9781119054450.ch3

Pons, T. L., Flexas, J., von Caemmerer, S., Evans, J. R., Genty, B., Ribas-Carbo, M., et al. (2009). Estimating mesophyll conductance to CO2: methodology, potential errors, and recommendations. *J. Exp. Bot.* 60, 2217–2234. doi: 10.1093/jxb/erp081

Ramírez, D. A., Yactayo, W., Rens, L. R., Rolando, J. L., Palacios, S., De Mendiburu, F., et al. (2016). Defining biological thresholds associated to plant water status for monitoring water restriction effects: Stomatal conductance and photosynthesis recovery as key indicators in potato. *Agric. Water Manage.* 177, 369–378. doi: 10.1016/j.agwat.2016.08.028

Reynolds-Henne, C. E., Langenegger, A., Mani, J., Schenk, N., Zumsteg, A., and Feller, U. (2010). Interactions between temperature, drought and stomatal opening in legumes. *Environ. Exp. Bot.* 68, 37–43. doi: 10.1016/j.envexpbot.2009.11.002

Richards, L. A. (1948). Porous plate apparatus for measuring moisture retention and transmission by soil. *Soil Sci.* 66. doi: 10.1097/00010694-194808000-00003

Rogers, A., Medlyn, B. E., Dukes, J. S., Bonan, G., von Caemmerer, S., Dietze, M. C., et al. (2017). A roadmap for improving the representation of photosynthesis in Earth system models. *New Phytol.* 213, 22–42. doi: 10.1111/nph.14283

Romero, A. P., Alarcón, A., Valbuena, R. I., and Galeano, C. H. (2017). Physiological assessment of water stress in potato using spectral information. *Front. Plant Sci.* 8. doi: 10.3389/fpls.2017.01608

Rouhi, V., Samson, R., Lemeur, R., and Damme, P. V. (2007). Photosynthetic gas exchange characteristics in three different almond species during drought stress and subsequent recovery. *Environ. Exp. Bot.* 13. doi: 10.1016/j.envexpbot.2005.10.001

Ryu, Y., Berry, J. A., and Baldocchi, D. D. (2019). What is global photosynthesis? History, uncertainties and opportunities. *Remote Sens. Environ.* 223, 95–114. doi: 10.1016/j.rse.2019.01.016

Sabot, M. E. B., De Kauwe, M. G., Pitman, A. J., Medlyn, B. E., Ellsworth, D. S., Martin-StPaul, N. K., et al. (2022). One stomatal model to rule them all? Toward improved representation of carbon and water exchange in global models. *J. Adv. Model. Earth Syst.* 14. doi: 10.1029/2021MS002761

Samaniego, L., Thober, S., Kumar, R., Wanders, N., Rakovec, O., Pan, M., et al. (2018). Anthropogenic warming exacerbates European soil moisture droughts. *Nat. Clim Change* 8, 421–426. doi: 10.1038/s41558-018-0138-5

Scoffoni, C., McKown, A. D., Rawls, M., and Sack, L. (2012). Dynamics of leaf hydraulic conductance with water status: quantification and analysis of species differences under steady state. *J. Exp. Bot.* 63, 643–658. doi: 10.1093/jxb/err270

Shi, X., and Bloom, A. (2021). Photorespiration: the futile cycle? *Plants* 10, 908. doi: 10.3390/plants10050908

Sorrentino, G., Haworth, M., Wahbi, S., Mahmood, T., Zuomin, S., and Centritto, M. (2016). Abscisic acid induces rapid reductions in mesophyll conductance to carbon dioxide. *PloS One* 11, e0148554. doi: 10.1371/journal.pone.0148554

Sperry, J. S., Venturas, M. D., Anderegg, W. R. L., Mencuccini, M., Mackay, D. S., Wang, Y., et al. (2017). Predicting stomatal responses to the environment from the optimization of photosynthetic gain and hydraulic cost: A stomatal optimization model. *Plant Cell Environ.* 40, 816–830. doi: 10.1111/pce.12852

Sprenger, H., Kurowsky, C., Horn, R., Erban, A., Seddig, S., Rudack, K., et al. (2016). The drought response of potato reference cultivars with contrasting tolerance. *Plant Cell Environ.* 39, 2370–2389. doi: 10.1111/pce.12780

Stirbet, A., Lazár, D., Guo, Y., and Govindjee, G. (2020). Photosynthesis: basics, history and modelling. *Ann. Bot.* 126, 511–537. doi: 10.1093/aob/mcz171

Tan, Z.-H., Wu, Z.-X., Hughes, A. C., Schaefer, D., Zeng, J., Lan, G.-Y., et al. (2017). On the ratio of intercellular to ambient CO2 (c i/c a) derived from ecosystem flux. *Int. J. Biometeorol* 61, 2059–2071. doi: 10.1007/s00484-017-1403-4

Théroux-Rancourt, G., Éthier, G., and Pepin, S. (2014). Threshold response of mesophyll CO2 conductance to leaf hydraulics in highly transpiring hybrid poplar clones exposed to soil drying. *J. Exp. Bot.* 65, 741–753. doi: 10.1093/jxb/ert436

Théroux-Rancourt, G., and Gilbert, M. E. (2017). The light response of mesophyll conductance is controlled by structure across leaf profiles. *Plant Cell Environ.* 40, 726–740. doi: 10.1111/pce.12890

Tholen, D., Boom, C., Noguchi, K., Ueda, S., Katase, T., and Terashima, I. (2008). The chloroplast avoidance response decreases internal conductance to CO_2 diffusion in *Arabidopsis thaliana* leaves. *Plant Cell Environ.* 31, 1688–1700. doi: 10.1111/j.1365-3040.2008.01875.x

Trenberth, K. E., Dai, A., van der Schrier, G., Jones, P. D., Barichivich, J., Briffa, K. R., et al. (2014). Global warming and changes in drought. *Nat. Clim Change* 4, 17–22. doi: 10.1038/nclimate2067

Urban, L., Aarrouf, J., and Bidel, L. P. R. (2017). Assessing the effects of water deficit on photosynthesis using parameters derived from measurements of leaf gas exchange and of chlorophyll a fluorescence. *Front. Plant Sci.* 8. doi: 10.3389/fpls.2017.02068

Valentini, R., Epron, D., Angelis, P., Matteucci, G., and Dreyer, E. (1995). *In situ* estimation of net CO2 assimilation, photosynthetic electron flow and photorespiration in Turkey oak (Q. cerris L.) leaves: diurnal cycles under different levels of water supply. *Plant Cell Environ.* 18, 631–640. doi: 10.1111/j.1365-3040.1995.tb00564.x

van Genuchten, M. (1980). A closed-form equation for predicting the hydraulic conductivity of unsaturated soils. *Soil Sci. Soc. America J.* 44, 892–898. doi: 10.2136/sssaj1980.03615995004400050002x

Veromann-Jürgenson, L.-L., Tosens, T., Laanisto, L., and Niinemets, Ü. (2017). Extremely thick cell walls and low mesophyll conductance: welcome to the world of ancient living! *J. Exp. Bot.* 68, 1639–1653. doi: 10.1093/jxb/erx045

Vidale, P. L., Egea, G., McGuire, P. C., Todt, M., Peters, W., Müller, O., et al. (2021). On the treatment of soil water stress in GCM simulations of vegetation physiology. *Front. Environ. Sci.* 9. doi: 10.3389/fenvs.2021.689301

Von Caemmerer, S. (2013). Steady-state models of photosynthesis: Steady-state models of photosynthesis. *Plant Cell Environ.* 36, 1617–1630. doi: 10.1111/pce.12098

Vos, J., and Oyarzún, P. J. (1987). Photosynthesis and stomatal conductance of potato leaves?effects of leaf age, irradiance, and leaf water potential. *Photosynth Res.* 11, 253–264. doi: 10.1007/BF00055065

Walker, B. J., and Ort, D. R. (2015). Improved method for measuring the apparent CO_2 photocompensation point resolves the impact of multiple internal conductances to CO_2 to net gas exchange: Photocompensation point measurements. *Plant Cell Environ.* 38, 2462–2474. doi: 10.1111/pce.12562

Wang, X., Du, T., Huang, J., Peng, S., and Xiong, D. (2018). Leaf hydraulic vulnerability triggers the decline in stomatal and mesophyll conductance during drought in rice. *J. Exp. Bot.* 69, 4033–4045. doi: 10.1093/jxb/ery188

Wang, Z., Li, G., Sun, H., Ma, L., Guo, Y., Zhao, Z., et al. (2018). Effects of drought stress on photosynthesis and photosynthetic electron transport chain in young apple tree leaves. *Biol. Open bio.*, 035279. doi: 10.1242/bio.035279

Wilson, K. B., Baldocchi, D. D., and Hanson, P. J. (2000). Quantifying stomatal and non-stomatal limitations to carbon assimilation resulting from leaf aging and drought in mature deciduous tree species. *Tree Physiol.* 20, 787–797. doi: 10.1093/treephys/20.12.787

Wong, S. C., Cowan, I. R., and Farquhar, G. D. (1979). Stomatal conductance correlates with photosynthetic capacity. *Nature* 282, 424–426. doi: 10.1038/282424a0

Xiao, Y., and Zhu, X. (2017). Components of mesophyll resistance and their environmental responses: A theoretical modelling analysis. *Plant Cell Environ.* 40, 2729–2742. doi: 10.1111/pce.13040

Xiong, D., Douthe, C., and Flexas, J. (2018). Differential coordination of stomatal conductance, mesophyll conductance, and leaf hydraulic conductance in response to changing light across species: Coordination of CO_2 diffusion and H_2O transport inside leaves. *Plant Cell Environ.* 41, 436–450. doi: 10.1111/pce.13111

Yin, X., and Amthor, J. S. (2024). Estimating leaf day respiration from conventional gas exchange measurements. *New Phytol.* 241, 52–58. doi: 10.1111/nph.19330

Zait, Y., and Schwartz, A. (2018). Climate-related limitations on photosynthesis and drought-resistance strategies of Ziziphus spina-christi. *Front. Forests Global Change* 1. doi: 10.3389/ffgc.2018.00003

Zhang, P., Yang, X., Manevski, K., Li, S., Wei, Z., Andersen, M. N., et al. (2022). Physiological and growth responses of potato (Solanum tuberosum L.) to air temperature and relative humidity under soil water deficits. *Plants* 11, 1126. doi: 10.3390/plants11091126

Zhou, S., Duursma, R. A., Medlyn, B. E., Kelly, J. W. G., and Prentice, I. C. (2013). How should we model plant responses to drought? An analysis of stomatal and non-stomatal responses to water stress. *Agric. For. Meteorology* 182–183, 204–214. doi: 10.1016/j.agrformet.2013.05.009

Zhou, H., Zhou, G., He, Q., Zhou, L., Ji, Y., and Lv, X. (2021). Capability of leaf water content and its threshold values in reflection of soil–plant water status in maize during prolonged drought. *Ecol. Indic.* 124, 107395. doi: 10.1016/j.ecolind.2021.107395

Zhu, K., Yuan, F. H., Wang, A. Z., Wu, J. B., Guan, D. X., Jin, C. J., et al. (2021). Stomatal, mesophyll and biochemical limitations to soil drought and rewatering in relation to intrinsic water-use efficiency in Manchurian ash and Mongolian oak. *Photosynt.* 59, 49–60. doi: 10.32615/ps.2020.084